Measurement of solid propellant ballistics by means of ultrasonic technique

A.N. Zayed[a], O. Kamal[a] and B. Lawton[b]
Military Technical College, Cairo, Eygpt
[b] Royal Military College of Science, England
e-mail: zayed_an01@hotmail.com

An ultrasonic pulse-echo technique is utilized to measure the burning rate of a composite solid propellant as a function of pressure. An evaluation of the measurement uncertainty of the method is also presented. Unlike the more traditional strand burner techniques, where dozens of constant pressure tests are necessary, the ultrasonic technique detects the position of the burning surface thousands of times per second as the pressure varies. This reduces the number of tests necessary to determine the ballistic characteristics of the solid propellant by one order of magnitude. This work presents new methods to characterize the changing speed of sound in the propellant and quantitative estimates of the measurement uncertainty in the burning rate measurement. The propellant samples were tested in a closed-combustion vessel, under pressurization rates of up to 158 Pa/s. The data obtained with the closed-combustion vessel tests using the ultrasonic method experimentally match with results of tests conducted in stand burners in steady-state condition.

يعرض هذا البحث طريقة إستخدام تقنية الموجات فوق الصوتية فى قياس معدل الإحتراق للوقود الصاروخى الصلب المركب وذلك كدالة فى ضغط الاحتراق. تم تقييم وتحليل لحيود نتائج هذه التجارب، كما تم تحديد دقة قياس كل متغير على حدا وتأثيرها على نتائج التجربة. وعلى عكس تقنيات المحارق التقليدية، فإن تقنية الموجات فوق الصوتية تحدد موضع سطح الإحتراق آلاف المرات فى الثانية الواحدة وذلك عند ضغوط مختلفة. هذا يؤدى إلى تقليل عدد التجارب المطلوبة لقياس الخصائص الباليستية للوقود الصاروخى الصلب. لإجراء هذه التجارب تم إحراق ستة عينات من الوقود الصاروخى المركب فى وعاء مغلق تحت ضغط إحتراق عالى حيث وصل معدل زيادة الضغط فى بعض التجارب إلى 158 ض.ج/ث. النتائج التى تم تسجيلها من هذه التجارب أورت موائمتها لنتائج التجارب التى تم إجرائها فى ظروف الاستقرار من ناحية ضغط الاحتراق.

Keywords: Solid propellant, Ballistic Coefficient, Ultrasonic measurement

1. Introduction

A solid rocket propellant is often evaluated using small samples in the laboratory. The end of the sample burns at a rate that is influenced by the gas pressure and the propellant formulation. The purpose of testing is to obtain the two coefficients "a" and "n" contained in Saint Robert's Law [1] (eq. (1)), which describes analytically the relation between the burning rate "r" and pressure "p":

$$r = a\, p^n. \tag{1}$$

This work demonstrates the use of a pulse-echo ultrasonic technique to determine the burning rate coefficients under transient pressure conditions and quantifies the measurement uncertainty.

The standard burner [2] has been the industry standard to determine the solid propellant burning rate because of its inherent simplicity. It consists of placing thin trip wires through strands of solid propellant that melt to interrupt an electric circuit. Dividing the distance between the wires by the time interval between the interruption of electrical continuity provides an average value of the burning rate. To determine the burning rate as a function of pressure requires a large number of constant pressure tests. Servo-mechanism methods [3], which use a motor controlled by an optical tracking feedback circuit to keep its reference position constant, have been developed since the late 1960s. The complex mechanisms and their ability to withstand exposure to hot, corrosive gasses reduce the utility of the approach. Microwave methods rely on measuring the reflected microwave off the surface of propellant. Although the system allows for a continuous measurement, it is still a relatively expensive

Alexandria Engineering Journal, Vol. 48 (2009), No. 6, 635-642

method and the interpretation of the data requires experience [4]. The gamma-rays and the computed tomography techniques were also utilized in burning rate measurement [5,6].

Ultrasonic measurement finds application in many fields of science and technology. Its most frequent use is in non-intrusive diagnostics. Examples are to find cracks within structures not visible from the surface, discontinuities in the bonding of components, and many other applications where non-destructive analysis of materials is favorably intended. The application of high-frequency acoustic waves in present work is not for these purposes, but to actually measure the surface position of burning propellant as a function of pressure, hence, the characteristics of the propellant ballistics are obtained.

The earliest applications of ultrasound to the measurement of the solid propellant burning rate in the United States were done by Hale [7] in 1967 and were brought to general attention by Wright [8] in 1969. Researchers at Orena [9] further refined the technique in the early 1970s. Over the past several years the work has addressed the variability of acoustic velocity in solid materials as a function of pressure [10], the effects of temperature [11], and the burning rate measurement under oscillatory pressure [12]. In this work a new method is presented to characterize the effect of pressure on acoustic velocity, make the first quantitative estimates of burning rate measurement uncertainty, and compare results with conventional methods.

2. Description of the ultrasonic technique

Fig. 1 shows an ultrasonic transducer used to emit an acoustic pulse that propagates up to the propellant surface where it is reflected. The same transducer has a built-in receiver that detects the reflected wave. A coupling material is placed between the transducer and the sample to provide a time delay so that the reflected signal is easily identified and to protect the transducer from the harsh environment within the combustion vessel. By measuring the propagation time, the instant-taneous thickness can be determined for each pulse. Also fig. 1 illustrates an example wave form as it appears on an oscilloscope. On the left side, it is easy to identify the emission peaks (1) followed by the peak associated with the internal reflection off the rear of the transducer (2). From the left, it is easy to identify the emission peaks (1) followed by the peak associated with the internal reflection off the rear of the transducer (2). The third peak (3) is the interface between the coupling material and the propellant. The last peak (4) is the echo coming from the surface of the propellant.

The propagation time is related to the material thickness and the speed of sound in the materials and expressed as [11].

$$\tau = \frac{2E_c}{C_c} + \frac{2E_p}{C_p}. \qquad (2)$$

where E_c is the thickness of the coupling material, E_p the thickness of the solid propellant sample, C_c and C_p are the speed of sound in the coupling material and solid propellant, respectively. Since the speed of sound in these materials is a function of pressure and temperature the effects have to be evaluated. The effect of pressure on the acoustic velocities in the materials is determined in pre-test and post-test calibrations. For the data presented here the temperature

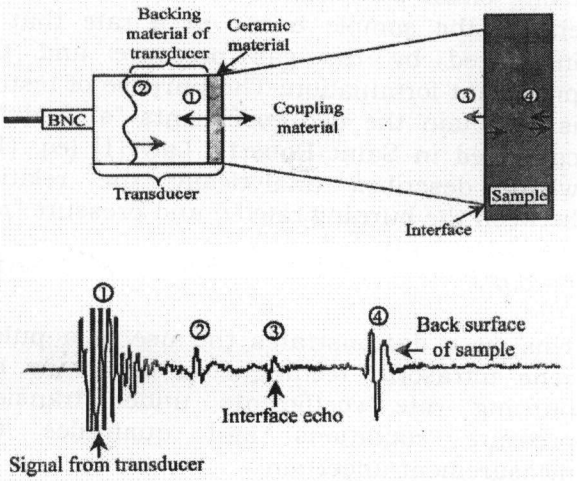

Fig. 1. Pulse-echo ultrasonic setup and typical signal.

profile effect was neglected. The temperature profile is an issue for propellants burning at low pressure with corresponding low thermal gradients at the surface [14].

The instantaneous thickness of the solid propellant "E_p" is meant to be calculated with this ultrasonic method. The data reduction algorithm acquires data from the propellant surface file, interface surface file, and firing data file. Subsequently, pressure calibration factors for the transducers, ultrasonic calibration points, and the initial propellant thickness are introduced into the data reduction algorithm. The calibration values are used to convert the voltage outputs of the pressure and ultrasonic transducers to calculate the pressure and return time.

With the data obtained from the pressurization tests, first-order regression coefficients "a_c" and "b_c" for the coupling materials and "a_p" and "b_p" for the solid propellant, are determined. With these four regression constants and the return time data of the firing test, the instantaneous length of the propellant can be determined as shown in eq. (3).

$$E_{p_k} = E_{prop}\frac{\tau_k(a_c p_k + b_c)}{(a_p p_k + b_p)}. \tag{3}$$

E_{prop} is the initial thickness of the solid propellant sample, p_k the pressure at the k-the point, and t_i is the test time. The burning rate is then obtained by finding the slope of a line fit through a number of points "N" before and after the point of interest. This process is repeated for each point. The number of points "N" is chosen to be large enough to eliminate the noise due to the discrete nature of the data but not so large to mask variations in the burning rate. Then, the instantaneous burning rate "r_k" is calculated as shown in eq. (4)

$$r_k = \frac{N\left(\sum_{i=k-N/2}^{i=k+N/2} E_{p_i} t_i\right) - \left(\sum_{i=k-N/2}^{i=k+N/2} E_{p_i}\right)\left(\sum_{i=k-N/2}^{i=k+N/2} t_i\right)}{\left(\sum_{i=k-N/2}^{i=k+N/2} t_i^2\right) - \left(\sum_{i=k-N/2}^{i=k+N/2} t_i\right)^2}. \tag{4}$$

3. Uncertainty analysis

To quantify the precision with which the measurement of the burning rate is determined, a detailed evaluation of the Uncertainty Magnification Factor (UMF) [13], and the Uncertainty Percentage Coefficient (UPC) [13], was done. The UMF is defined as

$$UMF_i = \frac{X_i}{r}\frac{\partial r}{\partial X_i}. \tag{5}$$

The *UMF* for a given variable X_i indicates the influence of the uncertainty in the variable with respect to uncertainty in the result "r". The *UPC* is defined as

$$UPC_i = \frac{\left(\frac{\partial r}{\partial X_i}\right)^2 (U_{X_i})^2}{U_r^2} \times 100. \tag{6}$$

The *UPC* for a given X_i gives the percentage contribution of the uncertainty in that variable to the squared uncertainty in the result. The *UMF* gives the sensitivity of the data reduction equation to the variables involved in the problem. The *UPC*, on the other hand, gives the actual weight of the uncertainty in the variable as a percentage of the total uncertainty. The instantaneous thickness of the solid propellant "E_p" is a function of pressure "p", propagation time "τ", the initial thickness of the solid propellant "E_{prop}", and the regression constants. In table 1, the variables uncertainties are summarized.

4. Instrumentation and experiments

4.1. Propellants

The composite propellant used in this investigation was the "Aerotech G12-RCT". The composition of that propellant is estimated at:

15% Hydroxyl-Terminated Polybutadiene (HTPB)

85% Ammonium Perchlorate (AP)

Table 1
Uncertainties in the variables

Variable	Uncertainty
p (MPa)	48.3
τ (μs)	1.0
E_{prop}	0.457
a_p	0.023%
b_p	3.548%
a_c	0.027%
b_c	2.794%

The propellant is cast as a tubular sample of 2.6 cm diameter and 6.9 cm long. The samples were prepared for the experiments by cleaving these propellant grains to the desired lengths. Initial weight and volume measurements gave an estimate of 1.6 g/cm^3 for the propellant density.

4.2. Combustion vessel

A scheme of the closed-combustion vessel used for these experiments is shown in fig. 2. It consists of a pressure vessel, a sample holder, and a pressurization system. The pressure vessel is made as a thick-walled stainless steel. Two electrical connectors provide a circuit path through the vessel wall to a pyrotechnic igniter. An upper cylindrical part is threaded on the top of the vessel containing the attachments for the pressure transducer and the inlet for the nitrogen pressurization and purge system.

The sample holder includes the propellant sample, epoxy, and an ultrasonic transducer. The sample holder allows acoustic access to the surface of propellant without having to expose the transducer to the harsh environment present in the vessel. The holder body is made from stainless steel and has a tapered cylindrical cavity in the center filled with epoxy resin. A cylindrically shaped propellant sample is glued on the top of the sample holder with the same resin. Epoxy is cast around the propellant to serve as an inhibitor and as a thermal barrier. Silicon grease is coated over the ultrasonic transducer to insure acoustic continuity. The ultrasonic transducer is mounted underneath the epoxy, as can be seen in fig. 2.

The top of the vessel is sealed with a burst disk. The burst disk provides a safety relief of the pressure if it rises above 38 GPa. The vessel can be pre-pressurized with nitrogen to a desired level, and thereafter the purge inlet is closed with a valve. The evaluation of the pressure and pressurization rate depends on:

- the burning surface area of the sample,
- the volume of the chamber,
- the burning rate of the propellant,
- the initial pressure in the chamber,
- the rate at which heat transferred through the wall.

4.3. Ultrasonic instrumentation

The equipment used for the ultrasonic measurement technique is a signal generator and converter manufactured by ONERA called the Electronic Device for Ultrasonic Measurement (EDUM) [15].

A Parametrics V102 1.0/1.0 ultrasonic transducer, a Tektronics 465 analog oscilloscope, and a National Instruments AT-MIO 16F 5 A/D board with LAB VIEW 4.0

The EDUM drives the ultrasonic transducer at 1 MHz, measure the propagation time "τ", and outputs a voltage proportional to τ. The device is capable of sampling at rates up to 20 kHz, but the data acquisition board used in this experiment was limited to 5000 Hz. A schematic example of the initial signal monitored on the oscilloscope prior to the test can be seen in fig. 3. As the propellant sample burns, the EDUM tracks the surface by locking on the first zero crossing echo 4. The coupling material serves the purposes stated earlier, but there are also advantages with regards to the ultrasonic measurement. First, it is a delay line so that the reflected echoes 3 and 4 arrive after the transducer ping 1 and back surface echo 2. Second, the use of epoxy resin allows for acoustic coupling of the transducer and the propellant. The acoustic impedance of the epoxy and propellant must match as closely as possible to minimize the propellant-epoxy interface echo. The lower trace (in fig. 3) shows the signal viewed after the sample has burned. The return time between echo 3 and echo 4 is proportional to the length of the sample. Data acquisition software completed the electronics arrangement.

The EDUM has an electronic circuit to generate two electronic masks. The purpose of the first mask is to cover both the decaying portion of the emission signal and the internal echoes of the transducer. The second mask serves to exclude any signals coming from beyond the peak associated with the burning surface of the propellant. The adjustment of the masks is obtained through raising or lowering of the threshold of the returned signal. An automatic gain control function maintains the amplitude of the received signal constant during the test. The signal is visualized on a HP54602B oscilloscope to insure for visual confirmation of the characteristics of the signal and the adjustment of the masks to increase the quality of the echoes. The data are simultaneously fed through the National Instruments Board connected to an ultra-sonic acquisition program that also acquires the data coming from the pressure transducer. A MATHCAD 7 worksheet is subsequently utilized, as shown in fig. 4, to reduce the data.

5. Experimental results and discussion

A test is composed of three phases. The first is a pressurization test without ignition consisting of opening the nitrogen feed valve of the closed vessel and allowing the pressure to rise up to the value found during combustion. This is necessary to measure the effect of pressure on the return time in the propellant and coupling material. The pressurization tests are repeated several times.

The firing test follows, where the propellant burns and the return time of the pulse-echo transducer as a function of pressure is obtained. The vessel is subseque ntly vented to allow the combustion gases to escape through the exhaust filtering system, and allowed to cool.

Once the vessel has reached room temperature, another pressuri-zation test is done to determine the speed of sound in the coupling material as a function of pressure. Fig. 5 illustrates the calibra-tion curves for the coupling material and propellant for test D table 2, as an example.

The initial conditions, maximum pressure, pressurization rates, regression constants, and the most important factors are the exponential factor "a" and the pressure exponent "n" obtained for the five tests conducted are summarized in table 2. or the first three tests in chronological order a Setra 5000-280E transducer was used, whereas for the last two tests a Setra 3000-280E transducer was used.

The results of the five tests conducted in the laboratory are superimposed in fig. 6. The test results are plotted on the same graph to emphasize the repeatability of the testing method. The analytical curve (thicker line) calculated with a pressure exponent "n" of 0.39 and a constant "a" of 0.023 [m/s Pa] given by the manufacture is also drawn in the figure. It is quite remarkable that the results are fitting close to each other.

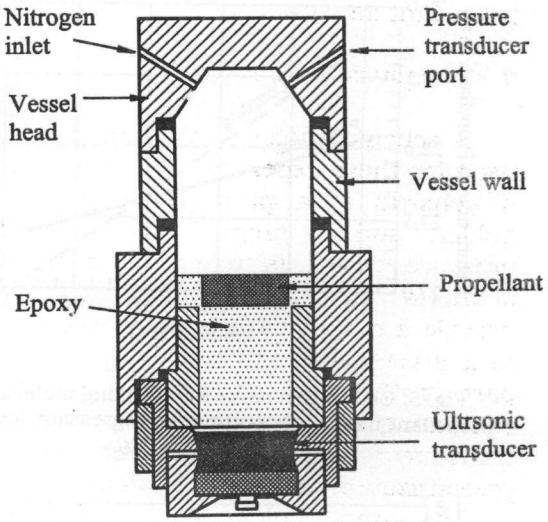

Fig. 2. Scheme of the closed-bomb combustion vessel.

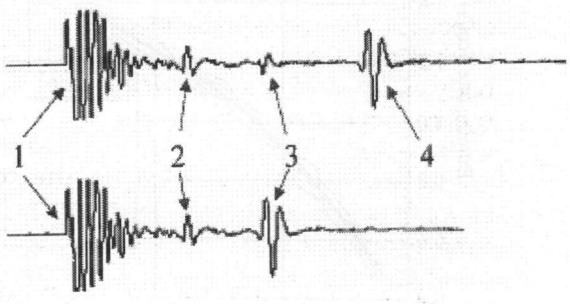

Fig. 3. Ultrasonic signal before and after the propellant sample has burned.

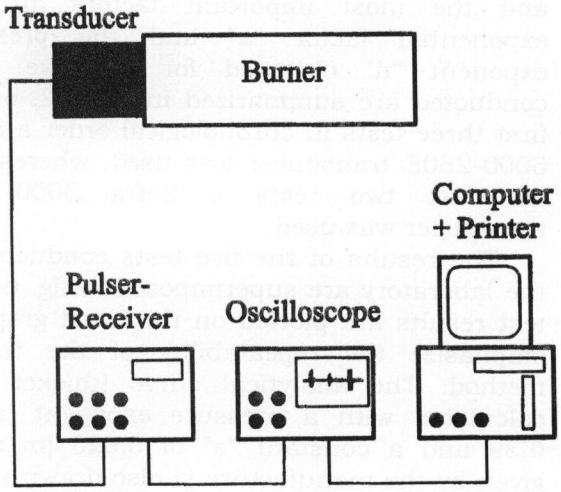

Fig. 4. Scheme of the experimental setup.

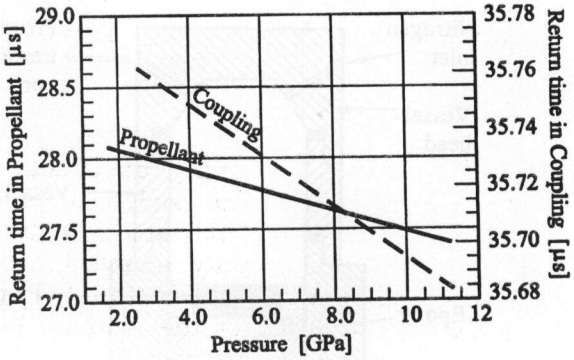

Fig. 5. Calibration curve for coupling material and propellant used to determine the regression coefficients a_c, b_c and a_p, b_p.

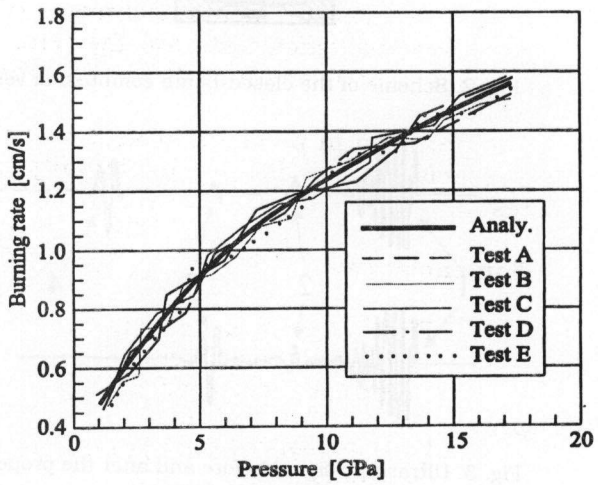

Fig. 6. Burning rates measured form tests overlapped with the curve calculated analytically.

Detailed uncertainty analysis tools have been developed. Here, it should be noted that the uncertainty is not only a general uncertainty of the method, but each test has its own uncertainty. The results, of the uncertainty analysis conducted on test D, are chosen for presentation as an example of all the tests conducted.

Test D had the greatest excursion in pressure. Fig. 7 illustrates the UMFs as a function in sample length for this test. The results for other tests are similar. As can be seen, the max. sensitivity is a consequence of the decrease in the length of the sample. The other variables influence the uncertainty with a coefficient of 1 or less. For UMFs equal to 1, the uncertainty in the variable propagates through the data reduction equation without being amplified.

In the case of pressure "p", where the UMF is of the order of 10^{-2}, uncertainties in pressure have negligible influence.

This is a surprising result, but the uncertainty analysis conducted on the data reduction [eq. (3)] shows an extremely high precision in pressure measurement. The measurement of the initial length of the sample is taken with great care to assure that the sample surface is plane. To achieve this, the samples are cut on a miter box to assure ends with right angle. If the sample is not square to within 1°, the sample has to be discarded.

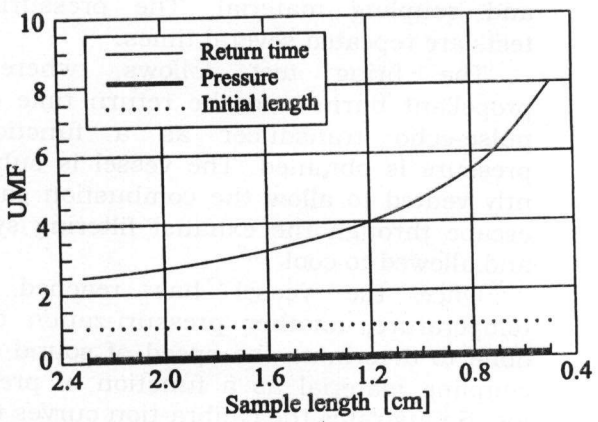

Fig. 7. UMF coefficients as a function of the sample length during the burn.

Table 2
Summary of the test conditions and results

	Test A	Test B	Test C	Test D	Test E
Conditions					
p_{init} (MPa)	715	1087	653	825	701
E_{init} (cm)	2.34	2.32	2.32	2.32	2.47
Results					
max p (MPa)	1.77×10^{4}	1.63×10^{4}	2.00×10^{4}	2.01×10^{4}	1.80×10^{4}
max $\Delta p/\Delta t$	1.29×10^{4}	1.25×10^{4}	1.59×10^{4}	1.39×10^{4}	1.24×10^{4}
a_c (μs/MPa)	-6.31×10^{-6}	-8.62×10^{-6}	-2.29×10^{-6}	-9.17×10^{-6}	-14.5×10^{-6}
b_c (μs)	36.63	35.91	36.08	35.79	39.34
a_p (μs/MPa)	-7.98×10^{-5}	-7.98×10^{-5}	-7.98×10^{-5}	-6.82×10^{-5}	-7.11×10^{-5}
b_p (μs)	29.34	28.97	29.14	28.19	26.89
a (cm/s MPa)	0.036	0.031	0.035	0.024	0.036
n	0.3841	0.3998	0.3887	0.4278	0.3810

The UPCs as a function of sample length are illustrated in fig. 8. It can be readily seen that the most sensitive measurement is that of the propagation time and it accounts for 60% of the uncertainty in the measurement of the instantaneous length E_p. The precision with which the initial sample length is measured accounts for 10% of the uncertainty in E_p, but it declines with the progression of the test. This result confirms the result of UMF analysis; the two most sensitive variables in the problem were the return time and the initial length of the propellant sample. The calculation of the UPCs confirms that the precision in the pressure measurement is not a crucial factor in result uncertainty.

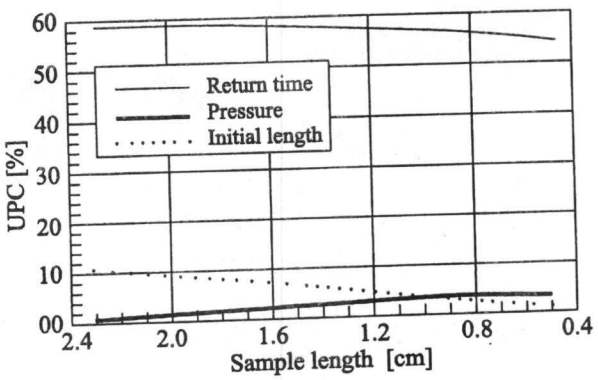

Fig. 8. UPC coefficients as a function of sample length during burning.

6. Conclusions

The measured burning rate of solid propellant is very close to the analytical value when measured at different burning pressures.

Detailed uncertainty analysis tools have been developed. The uncertainty here is not a general uncertainty of the method, but each test has its own uncertainty.

The UMF decreases with increasing the sample length, while the UPC decreases as the sample length decreases.

The two most sensitive variables in ultrasonic measurements technique of solid propellant ballistics tests are the return time and the initial length of the solid propellant sample.

The precision in pressure measurement is not a crucial factor in the uncertainty of the result.

Nomenclature

a	First ballistic coefficient,
b	Regression coefficient,
n	Second ballistic coefficient,
p	Combustion pressure,
r	Burning rate of solid propellant,
t	Test time,
C	Speed of sound,
E	Thickness,

N Number of points,
UMF Uncertainty magnification factor,
UPC Uncertainty percentage coefficient, and
τ Propagation time.

Subscript

c coupling,
p propellant, pressure, and
k instantaneous.

References

[1] B.L. Crawford and C. Huggett, "Propulsion Elements", National Research Committee Report (A-286) (1944).

[2] J.R. Osborn, R.J. Burick, and R.F. Panella, "Ballistic Measurement of Solid Propellant", Review Scientific Instrumentation, Vol. 37 (86) (1966).

[3] P. Kuentzmann and L. Nadaud, "Burning Rate Measurement of Solid Propellant in Closed Vessel", Combustion Scien-tific Technology, Vol. 11 (119) (1975).

[4] H.J. Hale, "Microwave Applications in Ballistics", M.Sc. Thesis, Virginia Polytechnic Institute (1967).

[5] A.N. Zayed and B. Lawton, "Measuring the Burning Rate in Solid Rockets by Using a Computed Tomography System", AIAA Paper 95-2594, 30-th AIAA Joint Propulsion Conference, San Diago, USA, Jul. (1995).

[6] A.N. Zayed, "Burning Rate Measurement in Solid Rockets by Means of a Pencil-like Gamma Ray Beam", 7th AMME (Applied Mechanics and Mechanical Engineering) International Conference, MTC, Cairo (1996).

[7] W.A. Wright, "Applications of the Ultra-Sound to the Measurement of the Solid Propellant Burning Rate", Aerospace Related Technology for Industry, NASA SP-5075 (National Aeronautics and Space Adminstration), 1969.

[8] P. Kuentzmann and F. Cauty, "Using Pulse-Echo Technique in Ballistics", Aerospace Technology, Vol. 1, No. 55, 1979.

[9] D. Deepak, R. Jeenu, and P. Sridharan, "Detection of Regression Rate by means of Ultrasonic Method", Journal of Propulsion and Power, Vol. 14 (29) (1998).

[10] P.A. Korting and H.F. Schoyer, "Heat Transfer in Fire and Combustion", ASME Conference, New York (1985).

[11] F. Cauty, "Ultrasonic Techniques in Com-bustion", ORENA Report (108) (1995).

[12] J. Louwers and D. Roekaerts, "Burning Rate Measurement Under Oscillatory Pressure", International Workshop on Measurement of Thermodynamics and Ballistics, Milano, Italy (1998).

[13] H.W. Coleman and W.G. Steele, "Experimentation and Uncertainty Analysis for Engineers" 2nd Edition, John Wiley and Sons, New York (1999).

[14] R. Di Salvo and F. Dauch, "Effects of Temperature Sensitivity of solid propellant on Burning Rate", 10-th Annual Propulsion Symposium, NASA Marshall Space Flight Center (1998).

[15] F. Cauty, "User's Manual of Electronic Device for Ultrasonic Measurement (EDUM) of Regression Rates of Solid Materials", France (1995).

Received March 1, 2009
Accepted August 23, 2009